1-1-2005

High-speed infrared phase modulators using short helical pitch ferroelectric liquid crystals

Ju-Hyun Lee
University of Central Florida

Dong-Woo Kim

Yung-Hsun Wu
University of Central Florida

Chang-Jae Yu

Sin-Doo Lee

Recommended Citation

Lee, Ju-Hyun; Kim, Dong-Woo; Wu, Yung-Hsun; Yu, Chang-Jae; Lee, Sin-Doo; and Wu, Shin-Tson, "High-speed infrared phase modulators using short helical pitch ferroelectric liquid crystals" (2005). *Faculty Bibliography 2000s*. 5387.
https://stars.library.ucf.edu/facultybib2000/5387

Authors

Ju-Hyun Lee, Dong-Woo Kim, Yung-Hsun Wu, Chang-Jae Yu, Sin-Doo Lee, and Shin-Tson Wu

High-speed infrared phase modulators using short helical pitch ferroelectric liquid crystals

Ju-Hyun Lee[1], Dong-Woo Kim[2], Yung-Hsun Wu[1], Chang-Jae Yu[2], Sin-Doo Lee[2], and Shin-Tson Wu[1]

[1]College of Optics and Photonics, University of Central Florida, Orlando, Florida 32816
[2]School of Electrical Engineering #32, Seoul National University, Kwanak, P.O.Box 34, Seoul 151-600, Korea
swu@mail.ucf.edu

Abstract: A fast phase modulator based on ferroelectric liquid crystal (FLC) is demonstrated and its performances characterized. For uniform alignment and pure phase modulation, we propose a new FLC device configuration using short helical pitch material and homeotropic alignment structure. This device is driven by periodic in-plane electrode stripes implemented on the surface of both cell substrates. As a result, we have obtained large phase modulation ($> 2\pi$ at λ=1.55 μm) and fast response (< 200 μsec).

OCIS codes: (160.3710) Liquid crystals; (230.3720) Liquid-crystal devices;

References and links

1. Y.-H. Wu, Y.-H. Lin, H. Ren, X. Nie, J. H. Lee, and S.-T. Wu, "Axially-symmetric sheared polymer network liquid crystals," Opt. Express, **13**, 4638-4644 (2005),
http://www.opticsexpress.org/abstract.cfm?URI=OPEX-13-12-4638
2. H. Ren, Y. H. Lin, Y. H. Fan, and S. T. Wu, "Polarization-independent phase modulation using a polymer-dispersed liquid crystal," Appl. Phys. Lett. **86**, 141110 (2005).
3. S. T. Wu and D. K. Yang, *Reflective Liquid Crystal Displays*, (Wiley, New York, 2001).
4. G. D. Love and R. Bhandari, "Optical properties of a QHQ ferroelectric liquid crystal phase modulator," Opt. Comm. **110**, 475-478 (1994).
5. J. Lagerwall, A. Saipa, F. Geisselmann, and R. Dabrowski, "On the origin of high optical director tilt in a partially fluorinated orthoconic antiferroelectric liquid crystal mixture," Liq. Cryst. **31**, 1175-1184 (2004).
6. R. B. Meyer, L. Liebert, L. Strzelecki, and P. Keller, J. Phys. Lett. **36**, L69-71 (1975).
7. I.-C. Khoo and S.-T. Wu, Optics and Nonlinear Optics of Liquid Crystals, (World Scientific, Singapore, 1993).
8. C. Wang, P. J. Bos, M. Wand, and M. Handschy, "A defect free bistable C1 SSFLC display," Soc. Inform. Display Tech. Digest,, **33**, 34-37 (2002).
9. N. A. Clark and S. T. Lagerwall, "Submicrosecond bistable electro-optic switching in liquid crystals," Appl. Phys. Lett. **36**, 899-901 (1980).
10. J. S. Patel, "Ferroelectric liquid crystal modulator using twisted smectic structure," Appl. Phys. Lett. **60**, 280-282 (1992).
11. L. A. Beresnev, L. M. Blinov, and D. I. Dergachev, "Electro-optical response of a thin layer of a ferroelectric liquid crystal with a small pitch and high spontaneous polarization," Ferroelectrics, **85**, 173-186 (1988).
12. L. A. Beresnev, V. G. Chigrinov, D. I. Dergachev, E. P. Poshidaev, J. Funfschilling, and M. Schadt, "Deformed helix ferroelectric liquid crystal displays: a new electrooptical mode in ferroelectric chiral smectic liquid crystals," Liq. Cryst. **5**, 1171-1177 (1989).
13. P. Rudquist, J. P. F. Lagerwall, M. Buivydas, F. Gouda, S. T. Lagerwall, N. A. Clark, J. E. Maclennan, R. Shao, D. A. Coleman, S. Bardon, T. Bellini, D. R. Link, G. Natale, M. A. Glaser, D. M. Walba, M. D. Wand, X.-H. Chen, "The case of thresholdless antiferroelectricity: polarization-stabilized twisted SmC* liquid crystals give V-shaped electro-optic response," J. Mater. Chem., **6**, 1257-1261 (1999).
14. S. S. Seomun, V. P. Panov, J. K. Vij, A. Fukuda, and J. M. Otón, "Dependence of the molecular orientational states on the surface conditions for the V-shape switching in ferroelectric-like samples", Phys. Rev. E **64**, 040701(R) (2001).
15. S.-S. Seomun, B. Park, A. D. L. Chandani, D. S. Hermann, Y. Takanishi, Ken Ishikawa, H. Takezoe, and A. Fukuda, "Langevin Type Alignment in a Smectic Liquid Crystal Mixture Showing V-Shaped Switching As Studied by Optical Second-Harmonic Generation," Jpn. J. Appl. Phys. **37**, L691- L693 (1998).

16. J.-H. Lee, C.-J. Yu, D.-H. You, and S.-D. Lee, "Wide-viewing display configuration of helix-deformed ferroelectric liquid crystals," Proc. Int'l Display Workshop, 129-132 (1999).
17. D.-H. You, S.-D. Lee, J.-H. Lee, and D. J. Na, "A dual in-plane electrode structure for better brightness in a helix-deformed FLCD," J. SID, **2**, 1-4 (2001).
18. S. J. Singer, "Layer buckling in smectic A liquid crystals and two-dimensional stripe phases," Phys. Rev. E, **48**, 2796-2804 (1993).
19. R. E. Geer, S. J. Singer, J. V. Selinger, B. R. Ratna, and R. Shashidhar, "Electric-field-induced layer buckling in chiral smectic-A liquid crystals," Phys. Rev. E. **57**, 3059-3062 (1998).

1. Introduction

High-speed phase modulation using liquid crystals (LCs) is desirable for photonic applications [1, 2]. Among various LC phases, nematic is widely used for displays, light shutters, and optical communications [3]. The major advantages of nematics are analog phase modulation capability and easiness of getting uniform molecular alignment. However, nematic is known to have slow response time because of the collective molecular reorientation. In addition, this slow response gets worse if the LC layer thickness increases in order to obtain a 2π phase change at an infrared wavelength, say $\lambda=1.55$ μm.

On the contrary, ferroelectric liquid crystals (FLCs) show very fast response time because their switching dynamics is different from that of nematic liquid crystals; it is based on the single-layered and cone-confined molecular switching mechanism. However, most of the FLC modes are not suitable for pure phase modulation devices because their optic axis sweeps in the plane parallel to the cell substrate so that it changes the polarization state of the incident light. To overcome the optic axis switching problem, a way of using a FLC as a phase modulator was reported by using a system consisting of a FLC half-wave plate sandwiched between two quarter-wave plates [4]. However, to achieve a 2π phase modulation, FLC's optic axis should be switched between 0 and 90 degrees. That is, FLC's smectic tilt angle should be 45 degrees and this value is hard to obtain in FLCs even it is realized in some antiferroelectric liquid crystals [5]. Moreover, many of them show the bistable switching that cannot be applied to the analog phase modulator. The most serious problem in FLC devices is that obtaining the alignment uniformity with optical quality is almost unattainable.

In this paper, we demonstrate a new FLC device configuration which shows a large phase modulation and fast response time. It also has good alignment uniformity with easy fabrication process.

2. Basic principles

Since the discovery of ferroelectricity in tilted chiral smectic liquid crystals, various FLC modes have been invented for optoelectronics and display applications [6, 7]. Because of FLCs' ferroelectricity and their microscopic structural characteristics, the electro-optical switching of FLC directors is described as a smectic cone confined rotational switching driven by the torque coming from coupling between the applied electric field and the polarization in FLC molecules. Therefore, to switch the FLC molecules efficiently, the electric field should be applied in parallel with the smectic layer.

Most of the FLC modes with planar alignment configuration in which smectic layers are almost perpendicular to the cell surfaces meet the above mentioned driving condition when the electric field is applied by the conventional two parallel electrodes on the surfaces of the bottom and the top substrates. However, in this configuration, there occurs a delicate surface interaction between the alignment surface and the FLC molecules; and, it makes the uniform alignment difficult.

A defect free surface-stabilized FLC (SSFLC) mode has been reported by using inorganic alignment layers [8]. However, the SSFLC mode is a bistable device [9]. On the contrary, some FLC modes show continuous gray scales such as twisted FLC mode [10], the deformed helix ferroelectric liquid crystal mode [11, 12], V-shaped thresholdless switching ferroelectric /anti-ferroelectric liquid crystal modes [13-15], etc. However, they are based on the planar

alignment structure and they have the in-plane switching optic axis. All of the above mentioned FLC modes are not suitable for the pure phase modulator.

Recently, a vertically aligned short-pitch FLC mode was suggested [16]. In this mode, the plane of optic axis switching perpendicular to the cell substrates looks like a vertically aligned nematic mode. This mode shows uniform alignment comparable to the uniformity of nematic liquid crystals. In addition, this mode maintains the fast response time and the gray scale capability, which are the major characteristics of short pitch FLCs.

The basic principle to achieve uniform alignment is related to the optical resolution of the incident light. If the helical pitch of FLC is much shorter than the wavelength of the incident light, the light cannot resolve the helical structure of the FLC. As a result, the polarization of the incident light is affected by the average optical property of FLC. In the case of homeotropic alignment of short pitch FLC, the smectic layers are parallel to the cell substrates. Thus the average optic axis is normal to the substrate surface and it is parallel to the helical axis when the driving signal is not applied. As a result, this mode looks like a vertically aligned NLC mode and shows a perfect dark state under crossed polarizers.

To operate this mode, the transverse electric field is required to be parallel to the cell surface. The electro-optic characteristics of this mode driven by conventional in-plane electrode structures on one side of the cell have been reported [16]. However, in that case, every other optic axis of the active region alternates because the voltage applied to the electrode stripes alternates. It induces fringe field near the edge of every electrode stripe. Because of its one-side electrode structure, transverse electric field strength decreases as it moves away from the electrode implemented side [17]. This situation forms a phase grating in the whole operating region and limits the large phase retardation. To solve these problems, in this paper, we implement the periodic in-plane electrode stripes on both surfaces of the top and the bottom substrates as shown in Fig. 1.

In this configuration, the electrode stripes are electrically connected by thin film resistor network. Because of the resistor network, the monotonous increasing/decreasing voltages are applied across the electrodes. In addition, the electrode patterns on both substrates are aligned precisely to hold the same voltage on the electrode stripes placed opposite to the substrates. Therefore, the equal-potential lines would align normally to the cell substrates and the uniform transverse electric field (E_x) can be obtained in certain range of the operating region. As a result, uniform phase retardation can be obtained in the operating region.
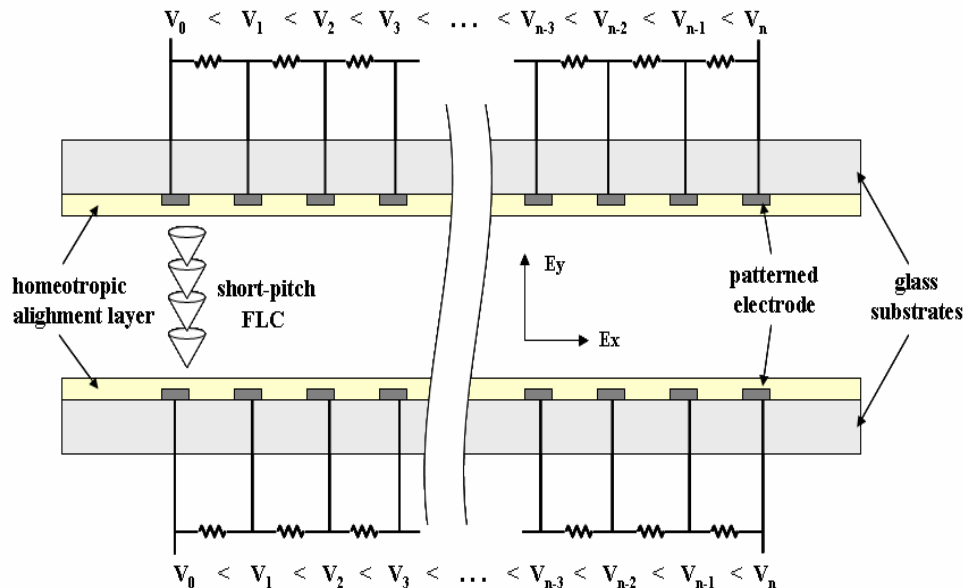

Fig. 1. Device structure for the phase modulator based on vertically aligned short-pitch FLC.

Figure 2 shows the simulation results of the above mentioned configuration. Figure 2(a) shows the potential distribution. The equal-potential lines are almost parallel to each other and normal to the cell substrate in the middle of the operating region. Constant strength of the transverse electric field (Fig. 2(b)) and almost zero vertical electric field (E_y) (Fig. 2(c)) are induced in this region. However, fringe fields remain near the edge of the operating region and they may affect the device performances.
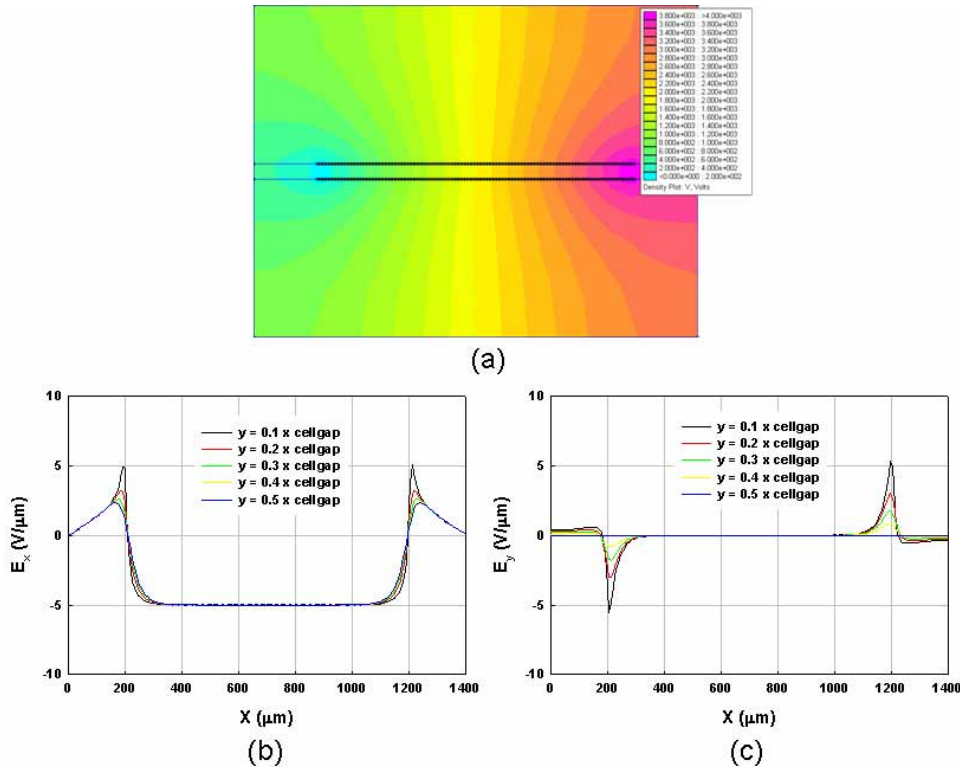

Fig. 2. Results of the electrostatic simulation for the suggested device configuration: distribution of (a) the electric potential, the electric field (b) parallel to the cell substrate, and (c) normal to the substrate.

3. Sample preparation

The FLC material used in this paper is FLC-10817, purchased from Rolic Technologies. Its phase transition has following sequence: isotropic (64.5~62.4^{o}C) $\rightarrow$ cholesteric (62.4 ~ 61.5^{o}C) $\rightarrow$ smectic C*. In the room temperature, the spontaneous polarization, the smectic tilt angle, and the helical pitch of FLC-10817 are 115 nC/cm^2, 34°, and less than 0.2 μm, respectively. The sample cell was made with glass substrates coated with patterned indium-tin-oxide electrodes. Polyimide JALS 204 (Japan Synthetic Rubber Co.) was coated on the substrate surfaces to promote homeotropic alignment. Neither surface was rubbed.

Comparing with the nematic vertical alignment (VA) mode, our vertically aligned FLC mode has a limit in the maximum switching angle of the optic axis. Nematic's optic axis switches the maximum angle of 90°. However, the average optic axis in our sample switches narrower than the smectic tilt angle. Therefore, the effective birefringence for normal incident light is reduced. To compensate for this effect and to obtain a large phase change, a thick LC layer is required. We have prepared two cells, one with 18 μm thick and the other with 50 μm.

Electrode pattern has a shape of periodically arranged stripes with 5 μm width and 10 μm intervals. Resistor network connects each electrode to the neighboring electrodes. The resistor

is made of n+ doped amorphous silicon coated by the plasma enhanced chemical vapor deposition process. The resistivity and the film thickness were controlled to apply the uniform interval of the voltage between neighboring electrode stripes. The electrode patterns on the bottom and the top substrates were aligned precisely by using a semiconductor aligner. UV curable epoxy was used to fix this pattern alignment in the cell assemble process.

The FLC mixture was injected into the cell using capillary effect in the isotropic phase. The cell was cooled slowly to achieve a uniformly aligned homeotropic texture. The temperature decreasing rate was 0.5°C/min and was controlled by a programmable furnace. Figure 3 shows the texture of FLC alignment observed by a polarizing microscope under parallel and crossed polarizer conditions. Even though the FLC cell gap is quite thick, we still obtained highly uniform alignment. Figure 3(a) shows the electrode stripes arranged in the diagonal direction. Darker part is the region where the electrodes are implemented on both substrates while the lighter part has only one side electrode pattern.
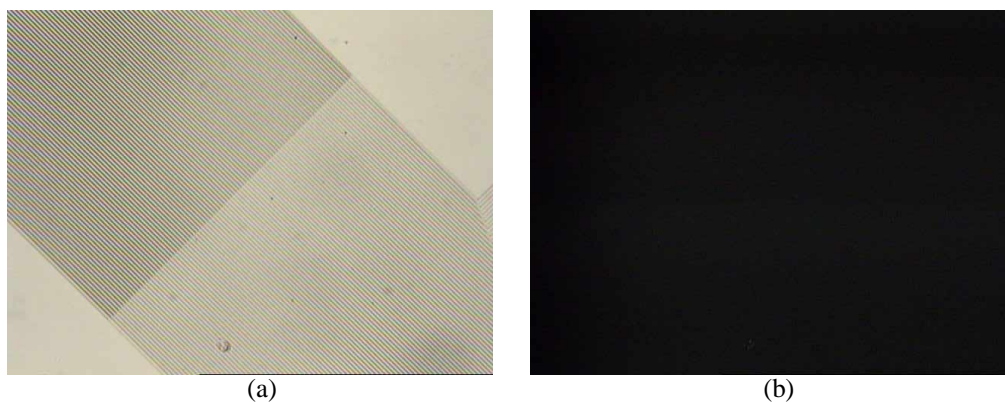

(a)   (b)

Fig. 3. Vertically aligned texture of short-pitch FLC observed by a polarizing microscope under (a) parallel and (b) crossed polarizer condition.

4. Experiment and results

At first, we observed the texture variation of the sample cell according to the driving voltage. Using a waveform generator and a voltage amplifier, we applied the driving signal of an AC square waveform to the sample. The maximum amplitude and the frequency of the driving signal were 200 volts and 60 Hz, respectively. To control the maximum electric field strength, we chose a pair of electrodes out of the electrode stripes and applied the driving voltage.

Figure 4 shows the LC texture photographs of the 18 μm thick cell under different driving voltages. In this case, we chose the zeroth and the tenth electrode. The distance between two electrode stripes is 100 μm so that the maximum 2 V/μm of transverse electric field (E_x) is applied in the middle of the operating region. The upper-left part of the operating region in the figure has electrodes on both substrates. The lower-right part has single side electrode pattern. Measurement was made in the upper-left part.

In the operating region, brightness and color are changed as the voltage increases. Textures are observed by using a polarizing microscope equipped with a white light source under crossed polarizer condition. Below 120 volts, only brightness is varied. Over 120 volts, however, color of the transmitted light is also changed. This result explains that the amount of the phase retardation is less than π for the wavelength of visible light when the driving voltage is below 120 volts. When the driving voltage is over 120 volts, the phase retardation is larger than π and the color aberration in the visible wavelength range cannot be neglected. This effect is also observed in the vertically aligned NLC cell with thick cell gap for more than π phase retardation.
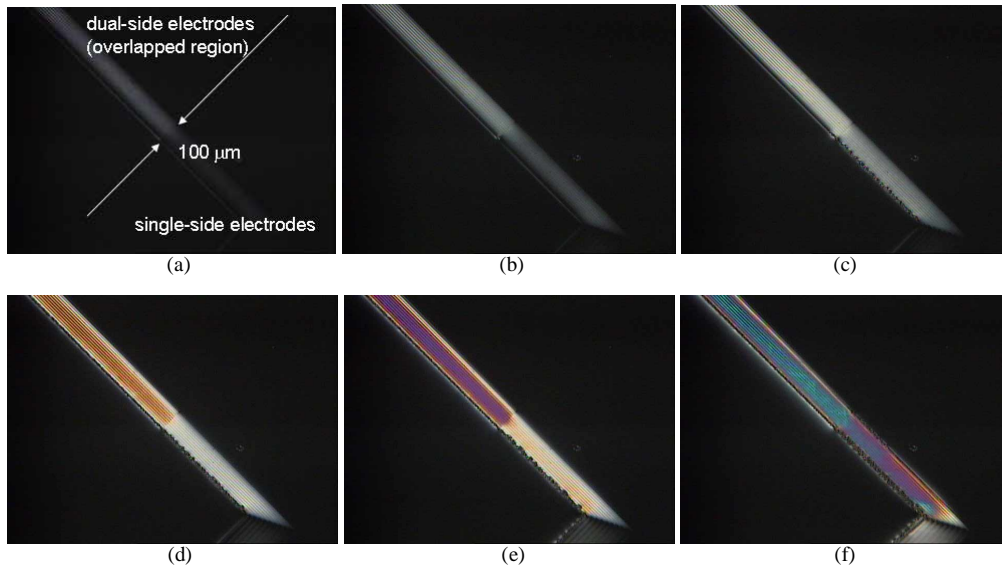
Fig. 4. Alignment texture variation according to the applied voltage change: (a) V_p=80, (b) 100, (c) 120, (d) 140, (e) 160, and (f) 200 volts, respectively.

Another important phenomenon in the result is the alignment breaking which occurs along the borders of the operating region. This effect takes place when the driving voltage is increased. Figure 5 shows the broken alignment. This broken alignment is not recovered by itself. However, we found that the thermal annealing can recover the alignment perfectly.

Next, we measured the voltage-dependent transmittance (V-T) curve. A He-Ne laser with λ=633 nm and a diode laser with λ=1.55 μm were used as probe beams. To avoid the effect of alignment breaking on the V-T curve, we used a convex lens to focus the laser beam and aligned the beam spot position to put it on the center of the operating region. When we measured the sample of 18 μm thick, we obtained less than 2π phase retardation for the He-Ne laser beam. At λ=1.55 μm, this value would be reduced by ~2.5X. Thus, the 18 μm cell does not have enough phase change for IR application.
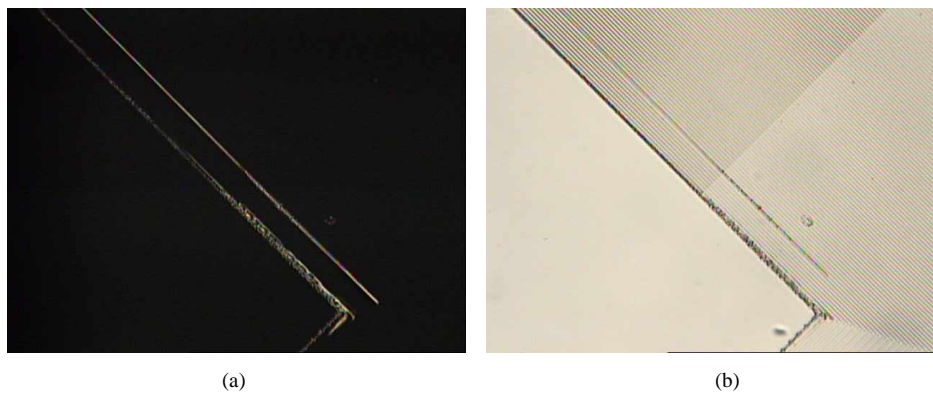

Fig. 5. Alignment breaking phenomenon occurs near the edge of the operating region. Photos are taken under (a) crossed and (b) parallel polarizer condition of a polarizing microscope.

We also measured the 50 μm sample using the λ=1.55-μm diode laser and obtained the result shown in Fig. 6. To increase the maximum transverse electric field strength, we applied the voltage to the fourth and the tenth electrode stripes. The maximum value of phase retardation was calculated from the normalized transmittance $T = \sin^2(\delta/2)$. The obtained

result is $\delta=2.3\pi$ at $\lambda=1.55$ μm and $E_x = 2.5$ V/μm. Above $E_x = 2.5$ V/μm, the alignment breaking worsens and permeates into the measurement region so that the V-T curve fluctuates severely.
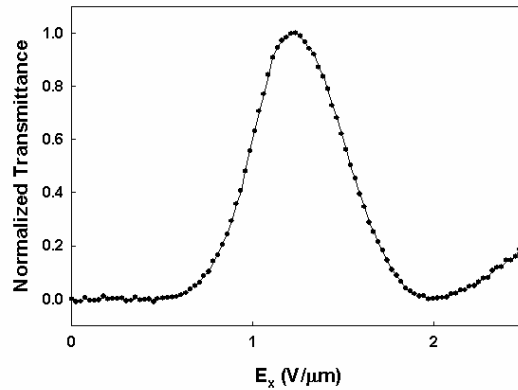

Fig. 6. Voltage dependent transmittance curve for the 50 μm thick sample driven by 60 Hz ac square field. Wavelength of the probe beam is $\lambda=1.55$μm.

Finally, we measured the response time of our device. To measure the turn-on (rise) and the turn-off (decay) time, we applied the unipolar square waveform of the driving voltage. Figure 7 shows the dynamic response of the 50 μm sample. The rise and the decay time are ~110 μsec and 60 μsec, respectively. When we measured the response time of the 18 μm sample, it is of the same order: the rise and the decay time are ~80 μsec and 60 μsec, respectively. From these results, we conclude that the response time of our device does not depend sensitively on the sample thickness and the electric field strength. This result is quite different from that of conventional FLC devices. Our helix-deformation-based vertical aligned FLC is supposedly free from the surface effect which affects the electro-optic response of the thin and planar FLC because our sample is driven by the lateral electric field and the FLC layer is relatively thick.
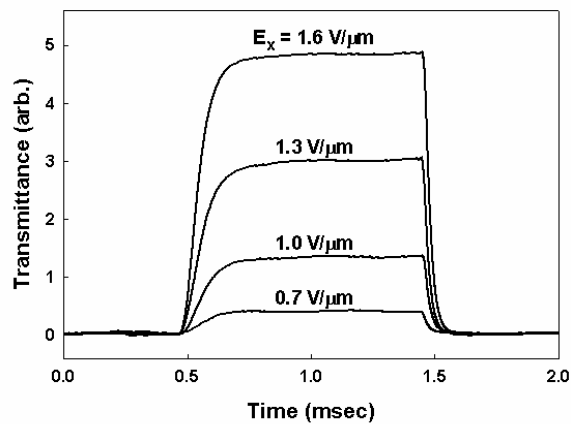

Fig. 7. Measured dynamic response of the vertically aligned short-pitch FLC sample. d=50μm and λ=633nm

5. Discussion

Unlike the conventional planar aligned FLC modes, one remaining problem in our device is the alignment breaking that occurs along the border of the operating region. The alignment breaking is supposed to come from the dielectric coupling between the negative dielectric anisotropy of the used material and the vertical electric field. For the verification of our assumption, we measured dielectric anisotropy of the used FLC. Using capacitance measurement method for the planar and the vertical aligned samples, we obtained the large value of negative dielectric anisotropy ($\Delta \varepsilon = \varepsilon_{vertical} - \varepsilon_{planar} \sim$ -23) in the frequency range of our measurement.

We also observed the texture variation of the thin sample that is driven by single side in-plane electrode structure. The other substrate has no electrode. The gap between the two electrodes was about 200 μm and the cell gap was 4.7 μm. Figure 8 shows the experimental results. Figures 8(a), (b), and (c) are textures under driving voltage of 80, 120, and 200 volts, respectively. Dark part is the region on the transparent electrode. The maximum strength of the transverse electric field (E_x) in the center region is about 1 V/μm when we applied 200 volts to the cell. This voltage is below the alignment breaking voltage. Because the electrodes are only on one substrate, the phase retardation is lower than that of the cell which has electrodes on both substrates [17]. Consequently, the experimental condition allows the low transmittance at the center of the operating region. On the contrary, it is observed that bright transmittance occurred close to the electrode edge. Considering the thin cell gap together with the weak electric field strength and the limit of the switching angle of the average optic axis, the bright transmittance is anomalous. This anomalous behavior is explained by the switching of the optic axis larger than smectic tilt angle by large dielectric coupling energy. However, the smectic layers tend to keep their thickness so that the dilative strain is induced along the direction normal to the smectic layer and it develops the layer modulation. This phenomenon is similar to the layer buckling in other layered systems [18, 19]. The prior studies were made with two-dimensional analysis. However, our case requires three-dimensional analysis because this effect is localized along the edge of the electrodes. This localized layer buckling seems to distort the un-buckled area in the operating region and induce a kind of hydrodynamic flow in the operating region as observed in Fig. 8. If this localized buckling is intensified further, continuum of the smectic layer between the buckled region and un-buckled region would not be sustained any longer; and, layer breaking is induced. This layer breaking brings about defects in the alignment texture. Theoretical study for the detailed analysis is in progress.
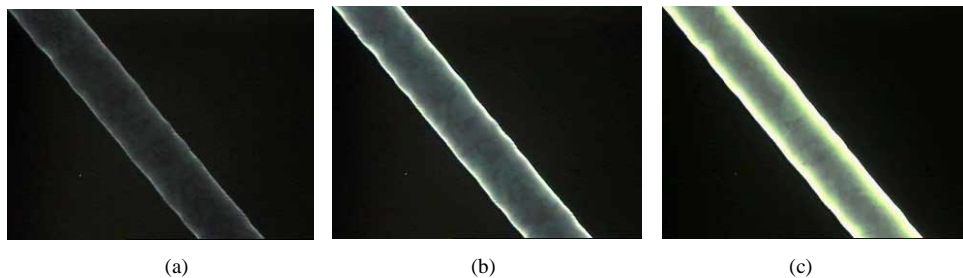

| (a) | (b) | (c) |

Fig. 8. Texture on the operating region of the vertically aligned FLC mode with single side in-plane electrode configuration driven by (a) 80 V, (b) 120 V, and (c) 200 V, respectively. Texture is observed by a polarizing microscope under crossed polarizer condition.

6. Conclusion

We have demonstrated a new FLC device structure based on the vertically aligned short-pitch FLC mode. Employing the in-plane electrode stripes which are implemented on the surface of both top and bottom substrates and electrically connected by the thin film resistor network,

fast response, large phase modulation with continuous gray scales have been obtained. In addition, good alignment uniformity is achieved by a simple fabrication process. It thus would be useful for photonic device applications such as a fast response spatial phase modulator. Further studies in relation to the optimization of the design parameters must be carried out to reduce the alignment breaking effect.

Acknowledgment